Kerr nonlinear switching in a hybrid silica-silicon microspherical resonator

F. H. Suhailin,[1,2] N. Healy,[1] Y. Franz,[1] M. Sumetsky,[3] J. Ballato,[4] A. N. Dibbs,[5] U. J. Gibson,[5] and A. C. Peacock[1*]

[1]*Optoelectronics Research Centre, University of Southampton, SO17 1BJ, United Kingdom*
[2]*School of Fundamental Science, Universiti Malaysia Terengganu, 21300 Kuala Terengganu, Malaysia*
[3]*Engineering and Applied Science, Aston University, B4 7ET, United Kingdom*
[4]*COMSET, School of Materials Science and Engineering, Clemson University, SC 29634, USA*
[5]*Department of Physics, Norwegian University of Science and Technology, 7491 Trondheim, Norway*
[*]*acp@soton.ac.uk*

Abstract: A hybrid silicon-core, silica-clad microspherical resonator has been fabricated from the semiconductor core fiber platform. Linear and nonlinear characterization of the resonator properties have shown it to exhibit advantageous properties associated with both materials, with the low loss cladding supporting high quality (*Q*) factor whispering gallery modes which can be tuned through the nonlinear response of the crystalline core. By exploiting the large wavelength shift associated with the Kerr nonlinearity, we have demonstrated all-optical modulation of a weak probe on the timescale of the femtosecond pump pulse. This novel geometry offers a route to ultra-low loss, high-*Q* silica-based resonators with enhanced functionality.

OCIS codes: (140.4780) Optical Resonator; (140.3948) Microcavity Devices; (160.6000) Semiconductor Materials.

References and links

1. D. W. Vernooy, A. Furusawa, N. Ph. Georgiades, V. S. Ilchenko, and H. J. Kimble, "Cavity QED with high-*Q* whispering gallery modes," Phys. Rev. A **57**, R2293−R2296 (1998).
2. A. M. Armani, R. P. Kulkarni, S. E. Fraser, R. C. Flagan, and K. J. Vahala, "Label-free, single-molecule detection with optical microcavities," Science **317**, 783−787 (2007).
3. J. U. Fürst, D. V. Strekalov, D. Elser, M. Lassen, U. L. Andersen, C. Marquardt, and G. Leuchs, "Naturally phase-matched second-harmonic generation in a whispering-gallery-mode resonator," Phys. Rev. Lett. **104**, 153901 (2010).
4. I. S. Grudinin and L. Maleki, "Ultralow-threshold Raman lasing with CaF_2 resonators," Opt. Lett. **32**, 166−168 (2007).
5. C. Y. Wang, T. Herr, P. Del'Haye, A. Schliesser, J. Hofer, R. Holzwarth, T. W. Hänsch, N. Picqué, and T. J. Kippenberg, "Mid-infrared optical frequency combs at 2.5 μm based on crystalline microresonators," Nat. Commun. **4**, 1345 (2013).
6. M. Borselli, K. Srinivasan, P. E. Barclay, and O. Painter, "Rayleigh scattering, mode coupling, and optical loss in silicon microdisks," Appl. Phys. Lett. **85**, 3693−3695 (2004).
7. L. Collot, V. Lefèvre-Seguin, M. Brune, J.-M. Raimond, and S. Haroche, "Very high-*Q* whispering-gallery mode resonances observed on fused silica microspheres," Europhys. Lett. **23**, 324−334 (1993).
8. F. Vanier, M. Rochette, N. Godbout, and Y.-A. Peter, "Raman lasing in As_2S_3 high-*Q* whispering gallery mode resonators," Opt. Lett. **38**, 4966−4969 (2013).
9. M. Pöllinger, D. O'Shea, F. Warken, and A. Rauschenbeutel, "Ultrahigh-*Q* tunable whispering-gallery-mode microresonator," Phys. Rev. Lett. **103**, 053901 (2009).
10. M. Pöllinger and A. Rauschenbeutel, "All-optical signal processing at ultra-low powers in bottle microresonators using the Kerr effect," Opt. Express **18**, 17764−17774 (2010).
11. W. Yoshiki and T. Tanabe, "All-optical switching using Kerr effect in a silica toroid microcavity," Opt. Express **22**, 24332−24341 (2014).
12. D. Farnesi, A. Barucci, G. C. Righini, S. Berneschi, S. Soria, and G. Nunzi Conti, "Optical frequency conversion in silica-whispering-gallery-mode microspherical resonators," Phys. Rev. Lett. **112**, 093901 (2014).

13. A. C. Peacock, J. R. Sparks, and N. Healy, “Semiconductor optical fibres: progress and opportunities,” Laser & Photonics Reviews **8**, 53−72 (2014).
14. J. Ballato, T. Hawkins, P. Foy, R. Stolen, B. Kokuoz, M. Ellison, C. McMillen, J. Reppert, A. M. Rao, M. Daw, S. Sharma, R. Shori, O. Stafsudd, R. R. Rice, and D. R. Powers, “Silicon optical fiber,” Opt. Express **16**, 18675−18683 (2008).
15. E. F. Nordstrand, A. N. Dibbs, A. J. Eraker, and U. J. Gibson, “Alkaline oxide interface modifiers for silicon fiber production,” Opt. Mater. Express **3**, 651−657 (2013).
16. N. Healy, J. R. Sparks, P. J. A. Sazio, J. V. Badding, and A. C. Peacock, “Tapered silicon optical fibers,” Opt. Express **18**, 7596−7601 (2010).
17. P. Wang, T. Lee, M. Ding, A. Dhar, T. Hawkins, P. Foy, Y. Semenova, Q. Wu, J. Sahu, G. Farrell, J. Ballato, and G. Brambilla, “Germanium microsphere high-*Q* resonator,” Opt. Lett. **37**, 728−730 (2012).
18. N. Vukovic, N. Healy, P. Mehta, T. D. Day, P. J. A. Sazio, J. V. Badding, and A. C. Peacock, "Thermal nonlinearity in silicon microcylindrical resonators," Appl. Phys. Lett. **100**, 181101 (2012).
19. L. Lagonigro, N. Healy, J. R. Sparks, N. F. Baril, P. J. A. Sazio, J. V. Badding, and A. C. Peacock, “Low loss silicon fibers for photonics applications,” Appl. Phys. Lett. **96**, 041105 (2010).
20. N. Vukovic, N. Healy, F. H. Suhailin, P. Mehta, T. D. Day, J. V. Badding, and A. C. Peacock., “Ultrafast optical control using the Kerr nonlinearity in hydrogenated amorphous silicon microcylindrical resonators,” Scientific Reports **3**, 2885 (2013).
21. T. V. Murzina, G. Nunzi Conti, A. Barucci, S. Berneschi, I. Razdolskiy, and S. Soria, “Kerr versus thermal non-linear effects studied by hybrid whispering gallery mode resonators,” Opt. Mater. Express **3**, 1088−1094 (2012).

1. Introduction

Efficient light-matter interactions in whispering gallery mode (WGM) microresonators with ultra-high quality (*Q*) factors and small mode volumes are of great interest for the development of compact and low power photonic devices. With an appropriate choice of cavity geometry and material, such resonators have found use in applications ranging from quantum electrodynamics [1] to biosensing [2]. In particular, for nonlinear applications, resonators fabricated from crystalline materials are often favored as their high nonlinear coefficients and low intrinsic losses reduce the power requirements [3,4,5]. However, the fabrication of micron-sized resonators from crystalline materials typically requires fairly labor-intensive processes such as mechanical polishing or multi-step etching to achieve high quality surfaces [4,6]. In contrast, resonators fabricated from micrometer sized glass fibers can be produced via a simple heating process that makes use of surface tension reshaping to form resonators with surface roughness values σ <1 nm [7,8]. Of these fiber resonators, much focus has been placed on devices that are fashioned from the extremely low loss silica platforms so that *Q* factors above 10^7 can be readily achieved [7,9]. Thus, despite silica’s relatively modest nonlinear coefficients, these ultra-high-*Q* resonators have still found use for nonlinear applications including all-optical switching [10,11] and third harmonic generation [12].

Over the past decade a new class of fiber has emerged that incorporates crystalline semiconductor materials into the core of a silica glass cladding [13]. Significantly, these hybrid fibers can be fabricated using conventional drawing techniques so that they retain many of the features of the standard fiber platforms that are favorable for the construction of high-*Q* resonators, such as the excellent mechanical integrity and pristine outer surfaces [14,15], but with the possibility to exploit the enhanced nonlinearity of the semiconductor core [13]. Furthermore, the robust glass cladding means that they can be post-processed to shape the core in order to introduce longitudinal variations that can be exploited for lateral light confinement [16]. For example, using a laser processing procedure to heat the end of a germanium core fiber, a spheroidal semiconductor resonator was formed that was completely encapsulated by the smooth glass cladding [17]. However, in this instance it was necessary to remove the rather thick cladding in order to access the semiconductor’s functionality, limiting the achievable *Q* factors and restricting the observation of any nonlinear effects.

In this paper, we present the first demonstration of a microspherical resonator shaped from the silicon fiber platform where it is possible to exploit the benefits of both the crystalline core and glass cladding materials. The resonator is still silica-based, i.e., the

circulating mode is confined by the pristine air/silica interface, but the highly nonlinear silicon core can be modulated to tune the resonances. In comparison to the pure silicon-based fiber resonators [18], this hybrid material resonator has a *Q* factor that is more than two orders of magnitude larger, which we attribute to the low loss cladding and improved coupling to the supported WGMs. To deconvolve the thermal and Kerr nonlinear contributions to the resonance wavelength red shift, a series of pump-probe measurements were performed using both continuous wave (CW) and pulsed sources. The large wavelength shift associated with the Kerr effect is confirmed by demonstrating its use for ultrafast all-optical modulation. Significantly, we believe that this is the first demonstration of Kerr-like modulation in a resonator where the nonlinear element is crystalline silicon.

2. Resonator fabrication and characterization

The hybrid microspherical resonator was formed from a silicon core, silica clad fiber that was fabricated via a modified drawing method described in [15]. Briefly, a silica tube (2 mm inner and 4 mm outer diameters) was coated with CaOH before packing with silicon powder. Here the role of the coating was to reduce thermal strain and act as a "sink" for impurities during the high temperature drawing. The constructed preform was then heated to ~1950 $^{\circ}$C using an oxyacetylene torch and, once the silicon is molten and the silica is softened, drawn into a silicon fiber at speeds of 1-2 m/s. The final fabricated fiber had an outer silica cladding diameter of ~82 μm with a ~50 μm silicon core. The linear loss value of the fiber (as made) was estimated via a simple transmission measurement to be ~11 dB/cm at 1550 nm, which is consistent with the expected polysilicon nature of the core material [15,19]. To introduce some spheroidal shaping into the fiber, a series of stable CO_2 laser pulses were focused onto the end of the fiber to soften the tip. A concentric sphere with a ~115 μm outer diameter and ~108 μm inner diameter was fabricated, as displayed in the microscope image of Fig. 1(a).

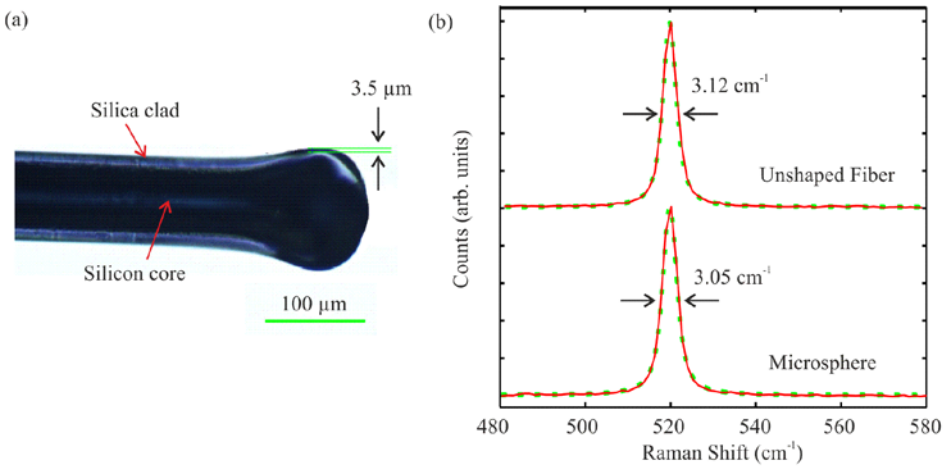

Fig. 1. (a) Microscope image of the hybrid microspherical resonator. (b) Raman spectrum of the polysilicon microspherical resonator core compared to that of the unshaped fiber core; solid lines are measured data, dotted curves are Voigt fits (Lorentzian linewidths as indicated).

In order to investigate the effects of the laser processing on the material quality of the core, Raman measurements were performed on the shaped and unshaped fiber, as shown in Fig. 1(b) [19]. Fitting these spectra, the estimated Lorentzian peak widths are found to be 3.05 cm^{-1} and 3.12 cm^{-1} for the shaped and unshaped core, respectively. Thus these results indicate that the material quality of the core was slightly improved by the reshaping, which is possibly due to the unprocessed core acting as a seed for the crystallization of the molten

silicon tip. However, in both cases the widths are larger than the single crystal reference (2.7 cm^{-1}), which is consistent with the polycrystalline nature of the material and the relatively high loss value of the starting fiber [19].

The set-up used to probe the optical properties of the resonator is illustrated in Fig. 2(a). An external tunable CW laser (Tunics Plus) that operates over the extended telecom band of 1.4-1.6 μm was coupled into WGMs via a tapered single mode fiber (SMF) with a waist diameter of 2 μm (see Box 1 in Fig. 2(a)). A polarization controller (PC) was placed before the taper to selectively couple into either the transverse electric (TE) or transverse magnetic (TM) WGMs. Micro-positioning stages were used to place the spherical resonator in close proximity to the taper to optimize coupling. The transmission spectrum plotted in Fig. 2(b) was measured via an optical component tester (OCT, Yenista CT 400 - Box 2), with a 1 pm resolution, and shows a series of resonance mode families that are excited with a free spectral range of FSR~ 4.7 nm. By fitting a Lorentzian curve to the resonance dip at λ_r ~1557.79 nm, as shown in the inset of Fig. 2(b), the full width half maximum (FWHM) linewidth was measured to be 0.014 nm, which yields a loaded quality factor of Q_l ~1.11 x 10^5. Significantly, this Q_l is two orders of magnitude larger than the values obtained for previous measurements conducted on pure silicon microcylindrical resonators (i.e., with no glass cladding) that have a similar bulk material quality [18]. We attribute the increased Q of our hybrid resonator to the fact that the WGMs are now largely confined within the silica cladding, which is both low loss and better suited to coupling from the tapered SMF, as well as the improved lateral confinement provided by the spherical shaping. It is worth noting that additional measurements conducted on an unshaped section of the fiber in Fig. 1(a) revealed Q_l ~4 x 10^4, which is still more than two times larger than the highest Q, pure silicon fiber-based resonators [20]. As a final comparison we also fabricated a pure silica microsphere with

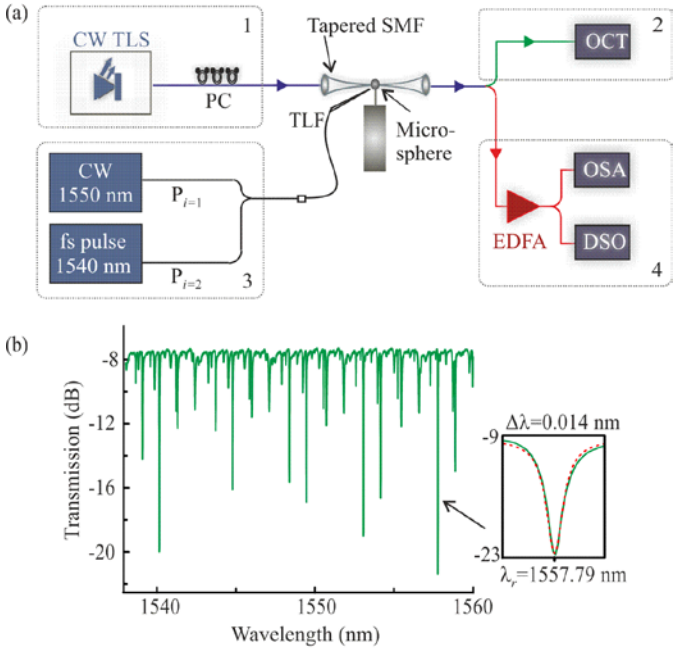

Fig. 2. (a) Set-up for characterizing the hybrid spherical resonators. Box 1 and 2 are used for the transmission measurements. Box 3 and 4 convert the set-up for the pump-probe experiments used to determine the nonlinear wavelength shifting for either a CW or pulsed pump. Polarization controller (PC), fiber amplifier (EDFA), tapered lens fiber (TLF), digital sampling oscilloscope (DSO), optical component tester (OCT). (b) Transmission spectrum. Inset: Lorentzian fit to determine Q_l.

the same outer diameter and a similar Q factor of Q_l ~1.55 x 10^5, from which we obtained a FSR of ~4.5 nm. The slightly larger FSR observed in the hybrid resonator indicates that the WGMs are interacting to some extent with the higher index silicon core.

3. Nonlinear characterization and ultrafast modulation

To investigate nonlinear tuning of the WGM resonances a pump-probe set-up was constructed using the components of Box 3 in Fig. 2(a). Here the pump is provided by one of the two sources, which are side-coupled to the hybrid resonator though a tapered lensed fiber (TLF) with a focused spot diameter of ~1 μm, allowing for tight focusing into the silicon core material. We note that in this configuration the pump was not required to be on-resonance, i.e., it was not launched into circulating mode. The different pump sources were chosen so that the effects of the thermal and Kerr nonlinearity could be deconvolved, where one is a low power CW diode at 1550 nm and the other is a high power femtosecond fiber laser at 1540 nm (720 fs FWHM duration and 40 MHz repetition rate). The resonance shift experienced by the weak probe was then monitored on the OCT (Box 2). For comparison, the spectrum of the pulsed pump was also monitored via the OSA (Box 4), from which it was possible to directly observe the wavelength at which the power is coupled to the resonator.

The size of the measured wavelength shift for the two sources is plotted in Fig. 3(a), where in both cases a linear red shift is observed as expected for the thermal and Kerr nonlinearities of silicon. For the CW source we obtained a maximum red shift of 0.10 nm for 27 mW of pump power coupled into the TLF, which we attribute entirely to the thermal nonlinearity associated with material absorption. In contrast, for the high peak power pulsed pump a shift of 0.32 nm was obtained for the same average power, so that we can attribute the additional shift to the Kerr effect [21]. To ensure that the observed shifting was due to the pump interacting with the silicon core, these measurements were repeated using the pure silica microsphere, where a maximum red shift of only ~0.05 nm was obtained for both pump sources. Although the power thresholds for the shifts observed in our hybrid resonator are higher than previously reported in the pure silicon resonators [20], this is a consequence of the off-resonance, side pumping geometry. Furthermore, for this scheme it is not possible to ascertain exactly how much of the pump light is coupled into the silicon core, so we can expect that the actual power required for this level of shifting will be lower. However, compared to coupling the pump into a resonator mode, side pumping does offer some key benefits as it removes the necessity for a precise pump wavelength and, as highlighted below, it is not limited by the resonance bandwidth.

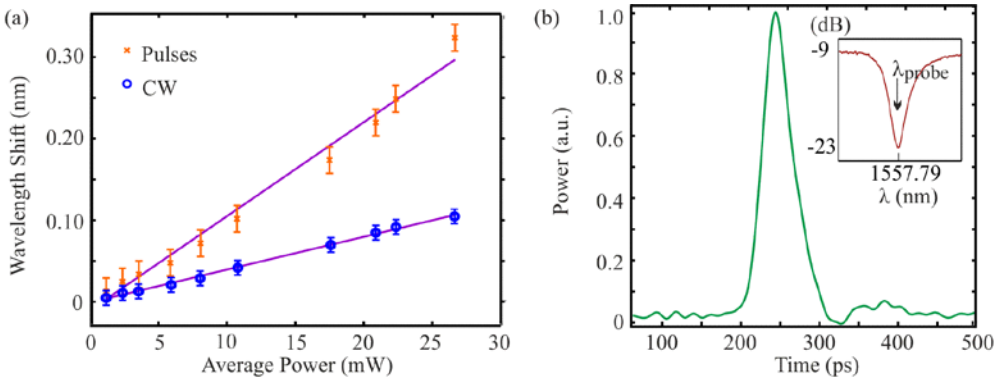

Fig. 3. (a) Wavelength shifting as a function of average power coupled into the TLF for CW and pulsed pumping. (b) All-optical switching of a CW probe induced by the pulsed pump. Inset: the CW probe position with respect to cold cavity resonance dip.

In order to verify the Kerr-like nature of the resonator response to the pulsed pump, the large wavelength shifting was exploited for ultrafast all-optical modulation. In this experiment we used the same set-up as employed to monitor the resonance shifting, except that now the tunable CW source is fixed to the wavelength of the cold cavity resonance, as indicated in the inset of Fig. 3(b). In this position the CW probe (~1 mW) is coupled into the resonance so that initially there is no light measured at the output of the taper. Figure 3(b) shows the subsequent switching on, then off of the probe associated with the ultrafast index change when the high power pump is present in the silicon core, as measured via a 30 GHz photodetector and digital sampling oscilloscope. This modulated signal was obtained for an average pump power of 10 mW, for which we recorded an extinction ratio of 5.9 dB. Unfortunately, owing to the bandwidth limitation of our measurement system only the impulse response of the high-speed on/off switching could be detected [20], so that it was not possible to fully resolve the temporal dynamics. Thus the result shown in Fig. 3(b) is the averaged signal pulse obtained by applying a low pass filter to remove the high frequency oscillations, which cleans up the response but also artificially broadens it in time. However, as for this off-resonance pumping scheme the Kerr index modulation will occur on the timescale of the 720 fs pump duration, we expect the on/off switching time to be sub-picosecond, which is an order of magnitude faster than previously reported in the pure silicon microcylindrical resonators [20].

4. Conclusion

We have fabricated and characterized the first hybrid silica/silicon microspherical resonator shaped from the silicon fiber platform. Our results have shown that these novel resonators exhibit advantageous properties associated with both materials, with the low loss silica cladding supporting coupling to high-*Q* WGMs which can be tuned through the nonlinear silicon core. By exploiting the large wavelength shift associated with the Kerr nonlinear response of the core, we have demonstrated ultrafast all-optical modulation on a timescale of the femtosecond pump pulse. To the best of our knowledge, this is the first demonstration of Kerr-based modulation obtained for a crystalline silicon-based resonator. Although the side pumping geometry necessitates that the power requirements for the modulation are relatively high, this could be addressed in future work through further optimization of the resonator geometry and pumping configuration. We expect that the enhanced functionality offered by these novel hybrid resonators will open up new avenues for compact, low loss, highly nonlinear optical devices.

Acknowledgments

The authors acknowledge EPSRC (EP/J004863/1), NORFAB (70201900/NL0133) and the Norwegian Discovery Fund (2011112) for financial support. M. Sumetsky is grateful to the Royal Society and Wolfson Foundation for his Royal Society Wolfson Research Merit Award. We also thank Dr L. Xiao for help with the resonator fabrication and characterization, and Dr P. Shardlow for assistance with the CO_2 laser cleaver. The data for this work is accessible through the University of Southampton Institutional Research Repository (DOI:10.5258/SOTON/377985).